Ground Deformation Spectra

GROUND DEFORMATION SPECTRA

T. Harada(I) and M. Shinozuka (II)

ABSTRACT

This paper presents a method of stochastically characterizing the spatial variabilities of earthquake ground motion and its resulting ground deformation for the purpose of the design and analysis of buried underunderground lifeline structures. The stochastic characterization is based on the theory of stochastic fields. The method is then applied to the analysis of dense seismic array data observed in Lotung, Taiwan. The notion of a ground deformation spectrum is also introduced.

INTRODUCTION

In contrast to the earthquake-resistant designs of above-ground structures where the inertial forces induced by ground acceleration are the main consideration, the spatial variation of the ground motion is of primary importance for buried lifeline structures such as pipelines and tunnels. Consistent with this observation, the response-displacement method was devised [1] and is widely used for the earthquake-resistant design of underground structures in Japan. However, the state-of-the-art of quantifying the spatial variability of earthquake ground motion and the permanent ground deformation resulting therefrom still leaves much to be desired.

In this context, presented herein is a method for characterizing the spatial variability of earthquake ground motion for the purpose of design on the basis of stochastic process theory. The method is then applied to the dense seismic array data observed in Lotung, Taiwan. The notion of a ground deformation spectrum is also introduced.

BACKGROUND

This section provides the fundamentals of the homogeneous time-space stochastic process theory focussing on the analytical as well as physical significance of the spatial correlation function. The fundamentals presented here are those associated with a uni-variate and spatially one-dimensional time-space stochastic process. However, an extension of the present work to problems involving multi-variate and multi-dimensional time-space stochastic processes can

I. Visiting Scientist, Columbia University; Associate Professor, Faculty of Engineering, Miyazaki University, Miyazaki, Japan.

II. Renwick Professor of Civil Engineering, Department of Civil Engineering and Engineering Mechanics, Columbia University, New York, NY.

be done. In fact, some work in this direction has been done at Miyazaki University [2] and at the Public Works Research Institute, Ministry of Construction, Japan [3] by interpreting the field data as sample functions of bi-variate and spatially two-dimensional time-space stochastic processes.

For a homogeneous time-space stochastic process $f(x,t)$ with zero mean, the time-space correlation function $Q(\xi,\tau)$ may be defined as

$$Q(\xi,\tau) = E[f(x+\xi,\ t+\tau)f(x,t)] \tag{1}$$

where $E[\cdot]$ represents the expectation operator. The quantities ξ and τ are the separation distance and time lag, respectively. Transforming the time lag τ into the frequency ω by means of the Wiener-Khintchine transform yields the temporal cross-spectral density function $P(\xi,\omega)$ as a function of ξ;

$$P(\xi,\omega) = \frac{1}{2\pi}\int_{-\infty}^{\infty} Q(\xi,\tau)e^{-i\omega\tau}d\tau \tag{2}$$

By performing an inverse transformation, one can reclaim $Q(\xi,\tau)$ as

$$Q(\xi,\tau) = \int_{-\infty}^{\infty} P(\xi,\omega)e^{i\omega\tau}d\omega \tag{3}$$

If the separation distance ξ is zero, the cross-spectral density function reduces to the two-sided point spectral density function (at any point x):

$$P(0,\omega) \equiv S_{ff}(\omega) \tag{4}$$

Normalization of the cross-spectral density function with respect to its value at $\xi = 0$ gives the frequency-dependent spatial auto-correlation function as follows,

$$r(\xi,\omega) = \frac{P(\xi,\omega)}{S_{ff}(\omega)} \tag{5}$$

The spatial auto-correlation function $R_{ff}(\xi)$ can be defined as $R_{ff}(\xi) = Q(\xi,0)$ and hence, with the aid of Eqs. 3 and 5,

$$R_{ff}(\xi) = Q(\xi,0) = \int_{-\infty}^{\infty} P(\xi,\omega)d\omega = \int_{-\infty}^{\infty} S_{ff}(\omega)r(\xi,\omega)d\omega \tag{6}$$

Thus, the spatial auto-correlation function is a weighted integral of the frequency-dependent spatial auto-correlation function $r(\xi,\omega)$ with the point spectral density function $S_{ff}(\omega)$ as the weight. If the time-space stochastic process is assumed to be ergodic, the spatial auto-correlation function may be estimated from the temporal average such that

$$R_{ff}(\xi) = Q(\xi,0) = \lim_{T\to\infty}\frac{1}{T}\int_0^T f^{(i)}(x+\xi,\ t)f^{(i)}(x,t)dt \tag{7a}$$

or from the following spatial average

$$R_{ff}(\xi) = Q(\xi,0) = \lim_{L\to\infty}\frac{1}{L}\int_0^L f^{(i)}(x+\xi,t)f^{(i)}(x,t)dx \tag{7b}$$

in which $f^{(i)}(x,t)$ represents the i-th sample function of $f(x,t)$. In practice, however, Eq. 7b cannot usually be used since the observations $f^{(i)}(x,t)$ are made at only a few discrete locations along the x-axis and therefore the integration of Eq. 7b is not possible.

RELATIVE DISPLACEMENT AND GROUND STRAIN

For the seismic design of buried pipelines, the maximum values of free-field ground strains and relative displacements between two points along the horizontal (x-) axis along which the pipeline would be buried become points of major interest. Hence, the analysis that follows primarily takes advantage of such spatially related statistics as the spatial auto-correlation function given by Eqs. 6 and 7, without specific use of frequency-dependent statistics at this time. The purpose of this section is to derive the basic relationships between the ground strains and relative ground displacements, on the basis of the stochastic process theory.

Consider the spatial variation of a free-field ground displacement along the x-axis. (Throughout the paper, the ground displacement and related quantities are those associated with a free field.) The ground displacement $u(x,t)$ at a given time instant t is assumed to constitute a homogeneous, univariate and one-dimensional stochastic field with zero mean and variance σ_u^2. Similarly, the ground strain $\varepsilon(x,t)$ is assumed to be a homogeneous, uni-variate and one-dimensional stochastic field with zero mean and variance σ_ε^2. For brevity of notation, they are denoted by $u(x)$ and $\varepsilon(x)$, dropping t in the argument.

Consider first the relative displacement $u_D(x)$ between x and x+D:

$$u_D(x) = u(x+D) - u(x) \tag{8}$$

Then, the auto-correlation function $R_{u_D u_D}(\xi)$ of $u_D(x)$ is given by

$$R_{u_D u_D}(\xi) = E[u_D(x+\xi)u_D(x)] \tag{9}$$

and can be shown to be

$$R_{u_D u_D}(\xi) = [2R_{uu}(\xi) - R_{uu}(\xi+D) - R_{uu}(\xi-D)] \tag{10}$$

where $R_{uu}(\xi)$ is the auto-correlation function of $u(x)$ with

$$R_{uu}(0) = \sigma_u^2 \tag{11}$$

Clearly, the variance of u_D is given by

$$\sigma_{u_D}^2 = R_{u_D u_D}(0) = 2[R_{uu}(0) - R_{uu}(D)] \tag{12}$$

Since $R_{uu}(D) \to 0$ as $D \to \infty$,

$$\sigma_{u_D}^2 = 2R_{uu}(0) = 2\sigma_u^2 \qquad \text{as } D \to \infty \tag{13}$$

On the other hand, $R_{uu}(D)$ can be expanded into the Taylor series around $D = 0$:

$$R_{uu}(D) = R_{uu}(0) + R'_{uu}(0)D + \frac{1}{2!}R''_{uu}(0)D^2 + \cdots \tag{14}$$

where $R'_{uu}(0) = dR_{uu}(\xi)/d\xi\big|_{\xi=0}$ and similar definitions apply to $R''_{uu}(0)$, etc. Due to the assumption that the free-field ground strain

$$u'(x) = \frac{du(x)}{dx} = \varepsilon(x) \tag{15}$$

is a homogeneous stochastic field with finite variance σ_u^2, or σ_ε^2, one obtains

$$2[R_{uu}(0) - R_{uu}(D)] = -R''_{uu}(0)D^2 = \sigma_\varepsilon^2 D^2 \qquad \text{as } D \to 0 \tag{16}$$

Making use of the apparent wave length L_u of the process $u(x)$,

$$L_u = 2\pi \frac{\sigma_u}{\sigma_\varepsilon} = 2\pi \sqrt{-\frac{R_{uu}(0)}{R''_{uu}(0)}} = 2\pi \sqrt{\frac{\int_{-\infty}^{\infty} S_{uu}(\kappa)d\kappa}{\int_{-\infty}^{\infty} S_{\varepsilon\varepsilon}(\kappa)d\kappa}} \tag{17}$$

one introduces the "correlation distance" L_u^* as

$$L_u^* = \frac{1}{\sqrt{2}\,\pi} L_u \tag{18}$$

and

$$\sigma_u = \frac{1}{\sqrt{2}} L_u^* \sigma_\varepsilon \tag{19}$$

Then, it follows from Eqs. 12, 16 and 19 that

$$\sigma_{u_D} = \sqrt{2}\,\frac{D}{L_u^*}\,\sigma_u \qquad \text{as } D \to 0 \tag{20}$$

In Eq. 17; $S_{uu}(\kappa)$ and $S_{\varepsilon\varepsilon}(\kappa)$ are the spectral density functions of $u(x)$ and $\varepsilon(x)$, respectively, and, in view of Eq. 15, $S_{\varepsilon\varepsilon}(\kappa)$ is related to $S_{uu}(\kappa)$ by

$$S_{\varepsilon\varepsilon}(\kappa) = \kappa^2 S_{uu}(\kappa) \tag{21a}$$

Parenthetically, it is noted that the spectral density function of $\varepsilon' = d\varepsilon(x)/dx$ is given by

$$S_{\varepsilon'\varepsilon'}(\kappa) = \kappa^4 S_{uu}(\kappa) \tag{21b}$$

which will be used later in the analysis. As is well known, $S_{uu}(\kappa)$ is in turn related to $R_{uu}(\xi)$ through the Wiener-Khintchine transform pair:

$$S_{uu}(\kappa) = \frac{1}{2\pi} \int_{-\infty}^{\infty} R_{uu}(\xi) e^{-i\kappa\xi} d\xi \tag{22a}$$

$$R_{uu}(\xi) = \int_{-\infty}^{\infty} S_{uu}(\kappa) e^{i\kappa\xi} d\kappa \tag{22b}$$

In Tables 1 and 2, two families of $R_{uu}(\xi)$ and $S_{uu}(\kappa)$ which are useful in the present analysis are listed.

Summarizing Eqs. 12, 13 and 20, one has

$$\sigma_{u_D} = \sqrt{2}\,\sqrt{R_{uu}(0) - R_{uu}(D)} \tag{23a}$$

$$= \sqrt{2}\,\frac{D}{L_u^*}\,\sigma_u \qquad \text{as } D \to 0 \tag{23b}$$

$$= \sqrt{2}\,\sigma_u \qquad \text{as } D \to \infty \tag{23c}$$

The significance of the correlation distance L_u^* is quite olear: The correlation distance L_u^* as defined for the purpose of this study is such that, when the relative distance D reaches the correlation distance L_u^*, the variance of the relative displacement becomes $2\sigma_u^2$ in accordance with Eq. 23b. This is the same variance of the relative displacement when u(x+D) and u(x) become completely uncorrelated as $D \to \infty$ (see Eqs. 23a and 23c).

Turning to the strain $\varepsilon(x)$, consider the local average $\varepsilon_D(x)$ of $\varepsilon(x)$ defined by

$$\varepsilon_D(x) = \frac{1}{D}\int_x^{x+D} \varepsilon(y)dy \tag{24}$$

which can also be written as

$$\varepsilon_D(x) = \frac{1}{D}\,u_D(x) \tag{25}$$

It follows then that

$$\sigma_{\varepsilon_D} = \frac{1}{D}\,\sigma_{u_D} \tag{26}$$

where $\sigma^2_{\varepsilon_D}$ is the variance of $\varepsilon_D(x)$. Recalling Eqs. 19 and 23 leads to

$$\sigma_{\varepsilon_D} = \frac{\sqrt{2}}{D}\sqrt{R_{uu}(0) - R_{uu}(D)} \tag{27a}$$

$$= \frac{\sqrt{2}}{L_u^*}\,\sigma_u = \sigma_\varepsilon \qquad \text{as } D \to 0 \tag{27b}$$

$$= \frac{\sqrt{2}}{D}\,\sigma_u = \frac{L_u^*}{D}\,\sigma_\varepsilon \qquad \text{as } D \to \infty \tag{27c}$$

Plotting σ_{u_D}/σ_u for the two limiting cases indicated in Eq. 23 as a function of D/L_u^* in a log-log scale, one obtains a diagram (heavy solid line) as shown in Fig. 1: From Eq. 23b,

$$\log\frac{\sigma_{u_D}}{\sigma_u} = \log\frac{D}{L_u^*} + \frac{1}{2}\log(2) \qquad D \le L_u^* \tag{28a}$$

and from Eq. 23c,

$$\log\frac{\sigma_{u_D}}{\sigma_u} = \frac{1}{2}\log(2) \qquad D \ge L_u^* \tag{28b}$$

Also, from Eq. 26,

$$\log \frac{\sigma_{u_D}}{\sigma_u} = \log \frac{D}{L_u^*} + \log\left(\frac{L_u^*}{\sigma_u}\sigma_{\varepsilon_D}\right) \tag{29}$$

Therefore, along a straight line making a 45° angle with the log (D/L_u^*) axis such as A in Fig. 1, the value of σ_{ε_D} is constant and hence, the average strain axis B can be constructed.

Four examples of the exact σ_{u_D} - D relationships (Eq. 23a) are plotted also in Fig. 1 (dashed curves) using the particular forms of the auto-correlation function designated as Types 1 and 2, respectively, in Tables 1 and 2 for $R_{uu}(\xi)/\sigma_u^2$. Observe that all these curves asymptotically approach the solid line in the ranges where $D \to 0$ and $D \to \infty$, and that in the intermediate range of D, the solid line tends to represent the average trend of all the dashed curves.

GROUND DEFORMATION SPECTRUM

While the σ_D - D relationship shown in Fig. 1 is of definite analytical interest, the relationship between max (u_D) and D will be more useful from the design point of view, where max (u_D) indicates the maximum value of $|u_D(x)|$ over length L along the x-axis. (This notation for max (u_D) will be used for other quantities throughout this paper.) The length L is the representative linear dimension of the area in which a network of pipelines of interest exist. Hence, the mathematical question here is: What is the absolute maximum value of the free-field relative displacement $u_D(x)$ as a function of D in a one-dimensional displacement field of u(x) over the range $0 \le x \le L$ where the auto-correlation function $R_{uu}(\xi)$ is known?

To answer this question, consider the apparent wave length L_{u_D} of $u_D(x)$ as

$$L_{u_D} = 2\pi \frac{\sigma_{u_D}}{\sigma_{u_D'}} = 2\pi\sqrt{\frac{R_{uu}(0) - R_{uu}(D)}{R_{\varepsilon\varepsilon}(0) - R_{\varepsilon\varepsilon}(D)}} \tag{30}$$

where $\sigma_{u_D'}^2$ is the variance of $u_D'(x)$ $(du_D(x)/dx)$ and $R_{\varepsilon\varepsilon}(\xi)$ is the auto-correlation function of $\varepsilon(x)$. Clearly, L_{u_D} is a function of the relative distance D. However, in the two limiting cases where $D \to 0$ and $D \to \infty$, L_{u_D} can be shown to take the following forms by the same reasoning as that used in deriving Eq. 21:

$$L_{u_D} = 2\pi \frac{\sigma_\varepsilon}{\sigma_{\varepsilon'}} = 2\pi\sqrt{-\frac{R_{uu}''(0)}{R_{uu}''''(0)}} = 2\pi\sqrt{\frac{\int_{-\infty}^{\infty} S_{\varepsilon\varepsilon}(\kappa)d\kappa}{\int_{-\infty}^{\infty} S_{\varepsilon'\varepsilon'}(\kappa)d\kappa}} = L_\varepsilon \qquad \text{as } D \to 0 \tag{31}$$

$$= 2\pi \frac{\sigma_u}{\sigma_\varepsilon} = 2\pi \sqrt{\frac{R_{uu}(0)}{R''_{uu}(0)}} = 2\pi \sqrt{\frac{\int_{-\infty}^{\infty} S_{uu}(\kappa)d\kappa}{\int_{-\infty}^{\infty} S_{\varepsilon\varepsilon}(\kappa)d\kappa}} = L_u \qquad \text{as } D \to \infty \qquad (32)$$

where L_u is the apparent wave length of $u(x)$, and L_ε the apparent wave length of $\varepsilon(x)$. In deriving Eq. 31, the existence of the variance of $\varepsilon'(x) = d\varepsilon(x)/dx$ has been assumed. Since L_u is generally larger than L_ε, L_{u_D} is approximately bounded by

$$L_\varepsilon \leq L_{u_D} \leq L_u \qquad (33)$$

By assuming the asymptotic largest value distribution function of the first type for max (u_D) and using its mode (most probable value) as the representative maximum for max (u_D), we define the peak factor PFA over the range $0 \leq x \leq L$ in the following form [4]

$$\frac{\text{Max}(u_D)}{\sigma_{u_D}} = \text{PFA} = \sqrt{2\ell n\left(\frac{2L}{L_{u_D}}\right)} \qquad (34)$$

Equation 34 is not valid unless $L >> L_{u_D}$. For small values of L, however, the mode of peak value distribution for the $u_D(x)$ process can be used as a conservative estimate of the representative maximum. To support this assertion, consider for example the limit as $L \to 0$. In this limit, max (u_D) has the same normal distribution as $u_D(x)$ itself has. On the other hand, the peak distribution function of $u_D(x)$ is located to the right of this normal distribution. Therefore, the mode of the peak distribution function of $u_D(x)$ is larger than the mode of the distribution function for max (u_D). This is a general trend that also applies to the case in which L is finite but small. Since the Rayleigh distribution function provides the most conservative mode, which is equal to σ_{u_D}, amongst the peak distribution functions having an identical standard deviation, σ_{u_D}, we assume that the PFA is bounded by unity from below for small values of L. Equation 34 implies that max (u_D) over length L along the x-axis can be obtained by multiplying σ_{u_D} by PFA (PEAK FACTOR). As mentioned above, the apparent wave length L_{u_D} of $u_D(x)$ varies between L_ε and L_u (Eq. 33) depending on the relative distance D. Therefore, the PFA given by Eq. 34 has the following approximate bounds:

$$\sqrt{2\ell n\left(\frac{2L}{L_u}\right)} \leq \text{PFA} \leq \sqrt{2\ell n\left(\frac{2L}{L_\varepsilon}\right)} \qquad (35)$$

From the design point of view, the upper bound PFA*

$$\text{PFA}^* = \sqrt{2\ell n\left(\delta \cdot \frac{2L}{L_u}\right)} \qquad (36)$$

is of more interest, where $\delta = L_u/L_\varepsilon$. However, in order to derive the upper bound, one must estimate L_ε. This requires knowledge of the auto-correlation function of the strain itself which in turn requires the derivative of u(x). Obviously, such information will not be available in practice. Alternatively,

L_ε can be obtained in terms of the second and fourth spectral moments of u(x) (see Eqs. 31 and 32). The spectral density function, however, can only be constructed through the Wiener-Khintchine transform of the auto-correlation function $R_{uu}(\xi)$ of u(x). Since at best $R_{uu}(\xi)$ can be estimated only in approximation and since the spectral moments can be highly sensitive to the analytical forms of the spectral density function $S_{uu}(\kappa)$, the alternative method of estimating L_ε also suffers from some uncertainty in the absence of a robust data base. Hence, it is recommended here that the following value be used for δ.

$$\delta = 2.5 \tag{37}$$

The value of δ in Eq. 37 was chosen from the following results, associated with particular forms of the auto-correlation function listed as Types 1 and 2 in Tables 1 and 2:

$$\delta = \frac{L_u}{L_\varepsilon} = \sqrt{6} = 2.5 \qquad \text{for Type 1 in Table 1} \tag{38a}$$

$$= \sqrt{5/2} = 1.6 \qquad \text{for Type 2 in Table 1} \tag{38b}$$

$$= \sqrt{3} = 1.7 \qquad \text{for Type 1 in Table 2} \tag{38c}$$

$$= \sqrt{5/3} = 1.3 \qquad \text{for Type 2 in Table 2} \tag{38d}$$

Note that Eq. 36 gives, in approximation, the lower bound of PFA when $\delta = 1$. In Fig. 2, the relationship between max (u_D) and D, the ground deformation spectrum, is plotted. This plot is obtained as follows: the dashed curves in Fig. 2 are obtained by multiplying the σ_{u_D} associated with the dashed curves in Fig. 1 by a PFA (Eq. 34), and the solid lines in Fig. 2 by multiplying the solid line in Fig. 1 by a PFA* with $\delta = 1.0$ and $\delta = 2.5$. Two sets of solid lines are obtained considering $L/L_u = 50$ in one case and $L/L_u = e/2 = 1.4$ for the other. Both the dashed curves and solid lines in Fig. 2 suggest that, for $D < L_u^*$, max (ε_D) may be used for max (ε).

The main thrust of this study lies in that (1) the absolute maximum relative ground displacement max (u_D) can be read from the ground deformation spectrum as constructed in Fig. 2, and (2) the max (ε_D) obtained from the spectrum can be used as max (ε). The apparent wave length L_u and the representative dimension L of the area in which the pipelines exist are the only quantities needed for the construction of such a spectrum. For design purposes, the maximum pipe strain can be estimated from max (ε), which is the maximum ground strain in a free field, if one multiplies it by a conversion factor β, for example, as defined by [5]. This approach by Shinozuka and Koike has in principle been adopted in the Seismic Design Guidelines for Gas Pipelines published by the Japan Gas Association (1982; in Japanese and for internal use only at this time).

ANALYSIS OF FIELD DATA

The preceding method is applied to the analysis of the dense seimic array data observed in Lotung, Taiwan. From the viewpoint of stochastic process theory, the field data are interepreted as a sample of a temporally and spa-

tially homogeneous stochastic process confined in a finite domain of temporal and spatial variables.

The data used in this analysis consist of the original accelerograms recorded on January 29, 1981 (Event 5) by the SMART-1 seismograph array installed at Lotung, Taiwan. These accelerograms have also been studied by others [6-8]. In particular, Bolt and Loh, and Harada showed that the strong portion of the accelerograms resulted from the wave propagating in the direction (x axis) of maximum variance with the angle $\phi = 64° - 86°$ (see Fig. 3). In this study, however, a displacement time history along the average direction ($\phi = 77°$ or N13°W) is computed at each accelerogram station from the two-component data (EW and NS).

Using these N13°W components of the ground displacements obtained from the accelerograms at sixteen stations (C00, I03 - I12, M03 - M09 and 004 - 007), the spatial auto-correlation values were computed and plotted (solid circles) in Fig. 4 upon normalization. Figure 4, however, involves only fifty-six relative distances appropriately chosen from all the possible combinations of the sixteen stations, two at a time. In this computation, the time window T = 10 sec was used in such a way that the strong portion of the seismic wave at each station was included in the window.

Similar computations were made for the same combinations of stations using the x directions with $\phi = 64°$ and 86° as the axes of projection. The results of these computations indicate that the correlation values change very little while the relative distances change significantly. This fact is demonstrated in Fig. 4 in terms of the range associated with each solid circle. The upper and lower bounds of each range correspond to the relative distances with respect to the directions of $\phi = 64°$ and 86° (not necessarily respectively, however).

The solid curve in Fig. 4 is an approximation for the sample spatial auto-correlation behavior and has the analytical form of Type 2 in Table 2,

$$R_{uu}(D) = \sigma_u^2\left\{1 - 2\left(\frac{D}{b}\right)^2\right\} \exp\left[-\left(\frac{D}{b}\right)^2\right] \tag{39}$$

with b = 1.131 km and σ_u = 1.3 cm. Using Eqs. 17 and 18, the apparent wave length and the correlation distance can be determined as $L_u = 2.9$ km and $L_u^* = 653$ m. Since the representative length L of the pipeline network is taken somewhat arbitrarily as L = 2.5 km in this study, the peak factor is obtained as PFA* = 1.3 from Eq. 36 with $\delta = 1.3$ corresponding to Eq. 39 (see Eq. 38d).

Making use of Eqs. 23a and 39 with the parameter values cited above and utilizing PFA* = 1.3, one obtains a ground deformation spectrum in the form of the solid curve in Fig. 5. In the same figure, the maximum relative ground displacements, associated with the same station pairs as used for the construction of Fig. 4 and measured from the field data directly, are plotted. The solid circles in Fig. 5 indicate the values of max (u_D) when the average azimuth direction is used as the axis of projection, while the bounds of the corresponding ranges indicate max (u_D) when the directions of $\phi = 64°$ and 86° are used as the axes. According to the solid curve in Fig. 5, max (ε_D) = 4×10^{-5} in this example and is valid for $D < L_u^* = 653$ m. As mentioned earlier, max (ε_D) can also be considered as max (ε) itself. The solid curve appears to

generally represent the relationship between max (u_D) and D directly measured from the field data, some scatter of data notwithstanding.

CONCLUSIONS

This paper presents a method of stochastically characterizing the spatial variabilities of free-field seismic ground motion and its resulting ground deformation for the purpose of the design and analysis of buried underground lifeline structures. The stochastic characterization is based on the theory of stochastic fields.

Time-space observations of ground displacement in a two-dimensional spatial domain are idealized as spatially uni-variate and one-dimensional waves propagating in the directions of maximum variance. On the basis of this idealization, an expression for the variance of the relative ground displacement at two spatial points is established as a function of the separation distance measured along these directions.

The absolute maximum value of the relative displacement in the spatial area of interest is then evaluated by multiplying the standard deviation of the relative displacement by a peak factor which depends on the representative linear dimension of the area as well as the apparent wave lengths of the ground displacement. This leads to the notion of a ground deformation spectrum.

Use of the ground deformation spectrum makes it possible that (1) the absolute maximum relative ground displacement be read from it and (2) the maximum average ground strain obtained from the spectrum can be used as the maximum ground strain itself. The apparent wave length of the ground displacement and the representative linear dimension of the area in which the pipelines exist are the only quantities needed for the construction of such a spectrum. For design purposes, the maximum pipe strain can be estimated from the maximum ground strain thus obtained, if one multiplies it by an appropriate conversion factor.

ACKNOWLEDGEMENT

The authors acknowledge the support provided by the Tokyo Gas Company, Ltd., Tokyo, Japan. Particular thanks are due to Mr. N. Nishio, Manager and Chief Researcher, Tokyo Gas Company, for his valuable comments on the tech-technical contents of this paper. Also, this work was partially supported by the National Science Foundation under Grant No. CEE-84-14205.

REFERENCES

(1) Kubo, K., Katayama, T. and H. Ohashi, "Lifeline Earthquake Engineering in Japan," Journal of the Technical Councils, ASCE, Vol. 105(TC1), 221-238, 1979.

(2) Harada, T. and T. Oda, "Probabilistic Analysis of Seismic Array Data with Application to Lifeline Earthquake Engineering," Memoirs of the Faculty of Engineering, Miyazaki University, Vol. 15, 1985.

(3) Harada, T. et al., "Preliminary Study on Spatial Variation of Ground Deformation for Seismic Design of Buried Lifeline Structures," Public Works Research Institute Report No. 2143, Ministry of Construction, 1984 (in Japanese).

(4) Longuet-Higgins, M.S., "On the Statistical Distribution of the Heights of Sea Waves," Journal of Marine Research, Vol. 11(3), pp. 245-266, 1952.

(5) Shinozuka, M. and T. Koike, "Estimation of Structural Strains in Underground Lifeline Pipes," Proceedings of the 3rd National Congress on Pressure Vessels and Piping, San Francisco, California, June 25-29, 1979, edited by T. Ariman, S-C. Liu and R.E. Nickell, 31-48.

(6) Bolt, B.A. et al., "Preliminary Report on the SMART-1 Strong Motion Array in Taiwan," No. EERC-82/13, University of California, Berkeley, 1982.

(7) Harada, T., "Probabilistic Modeling of Spatial Variation of Strong Earthquake Ground Displacements," Proceedings of the 8th World Conference on Earthquake Engineering, pp. 605-612, 1984.

(8) Vanmarcke, E.H. and R.S. Harichandran, "Models of the Spatial Variation of Ground Motion for Seismic Analysis of Structures," Proceedings of the 8th World Conference on Earthquake Engineering, pp. 597-604, 1984.

Table 1 AUTO-CORRELATION AND SPECTRAL DENSITY FUNCTIONS

Type	$R(\xi)$	$S(\kappa)$
1	$\frac{b^2}{\xi^2+b^2}$	$\frac{1}{2\cdot 0!} be^{-b\|\kappa\|}$
2	$\frac{b^4(b^2-3\xi^2)}{(\xi^2+b^2)^3}$	$\frac{1}{2\cdot 2!} b^3\kappa^2 e^{-b\|\kappa\|}$
3	$\frac{b^6(b^4-10b^2\xi^2+5\xi^4)}{(\xi^2+b^2)^5}$	$\frac{1}{2\cdot 4!} b^5\kappa^4 e^{-b\|\kappa\|}$
4	$\frac{b^8(b^6-21b^4\xi^2+35b^2\xi^4-7\xi^6)}{(\xi^2+b^2)^7}$	$\frac{1}{2\cdot 6!} b^7\kappa^6 e^{-b\|\kappa\|}$
5	$\frac{b^{10}(b^8-36b^6\xi^2+126b^4\xi^4-84b^2\xi^6+9\xi^8)}{(\xi^2+b^2)^9}$	$\frac{1}{2\cdot 8!} b^9\kappa^8 e^{-b\|\kappa\|}$
6	$\frac{b^{12}}{(\xi^2+b^2)^{11}} \times (b^{10}-55b^8\xi^2+330b^6\xi^4-462b^4\xi^6+ + 165b^2\xi^8-11\xi^{10})$	$\frac{1}{2\cdot 10!} b^{11}\kappa^{10} e^{-b\|\kappa\|}$

Table 2 AUTO-CORRELATION AND SPECTRAL DENSITY FUNCTIONS

Type	$R(\xi)$	$S(\kappa)$
1	$e^{-(\frac{\xi}{b})^2}$	$\frac{1}{2}\cdot\frac{b}{\sqrt{\pi}} \exp[-(\frac{b\kappa}{2})^2]$
2	$[1-2(\frac{\xi}{b})^2]e^{-(\frac{\xi}{b})^2}$	$\frac{1}{2}\cdot\frac{b^3}{2\sqrt{\pi}} \kappa^2\exp[-(\frac{b\kappa}{2})^2]$
3	$[1-4(\frac{\xi}{b})^2+\frac{4}{3}(\frac{\xi}{b})^4]e^{-(\frac{\xi}{b})^2}$	$\frac{1}{2}\cdot\frac{b^5}{12\sqrt{\pi}} \kappa^4 \exp[-(\frac{b\kappa}{2})^2]$
4	$[1-6(\frac{\xi}{b})^2+4(\frac{\xi}{b})^4-\frac{8}{15}(\frac{\xi}{b})^6]e^{-(\frac{\xi}{b})^2}$	$\frac{1}{2}\cdot\frac{b^7}{120\sqrt{\pi}} \kappa^6\exp[-(\frac{b\kappa}{2})^2]$
5	$[1-8(\frac{\xi}{b})^2+8(\frac{\xi}{b})^4-\frac{32}{15}(\frac{\xi}{b})^6+\frac{16}{105}(\frac{\xi}{b})^8]e^{-(\frac{\xi}{b})^2}$	$\frac{1}{2}\cdot\frac{b^9}{1680\sqrt{\pi}} \kappa^8\exp[-(\frac{b\kappa}{2})^2]$
6	$[1-10(\frac{\xi}{b})^2+\frac{40}{3}(\frac{\xi}{b})^4-\frac{16}{3}(\frac{\xi}{b})^6+\frac{16}{21}(\frac{\xi}{b})^8-\frac{32}{945}(\frac{\xi}{b})^{10}]e^{-(\frac{\xi}{b})^2}$	$\frac{1}{2}\cdot\frac{b^{11}}{30240\sqrt{\pi}}\kappa^{10}\exp[-(\frac{b\kappa}{2})^2]$

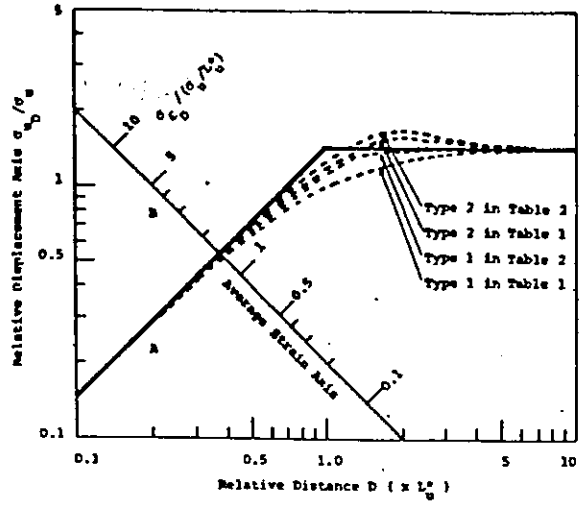

Fig. 1 σ_{u_D} – D Diagrams for Various Spatial Correlation Functions and Their Approximation

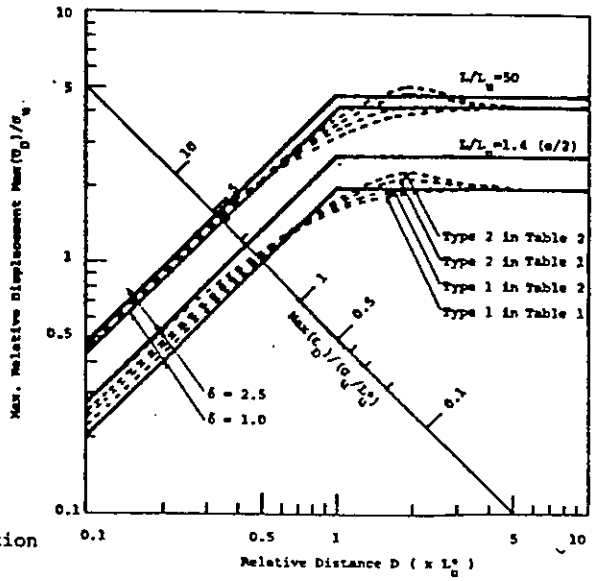

Fig. 2 Ground Deformation Spectra Associated with Various Spatial Correlation Functions and Their Approximation

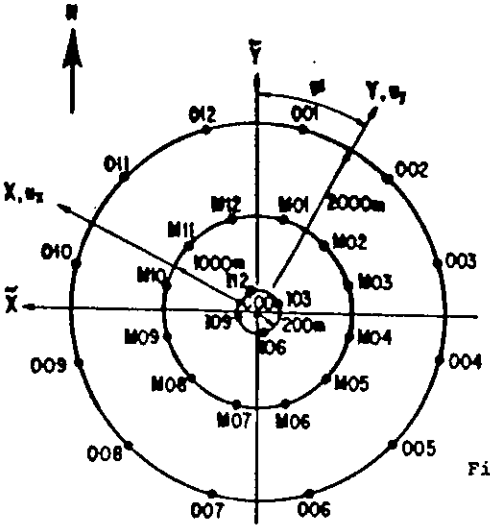

Fig. 3 The SMART-1 Array and Coordinate System

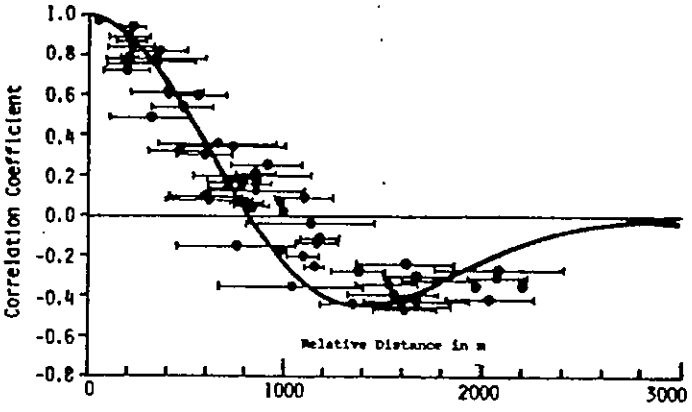

Fig. 4 Sample Spatial Correlation Coefficients and Approximated Correlation Function (N13°W Displacement, SMART-1, Event 5)

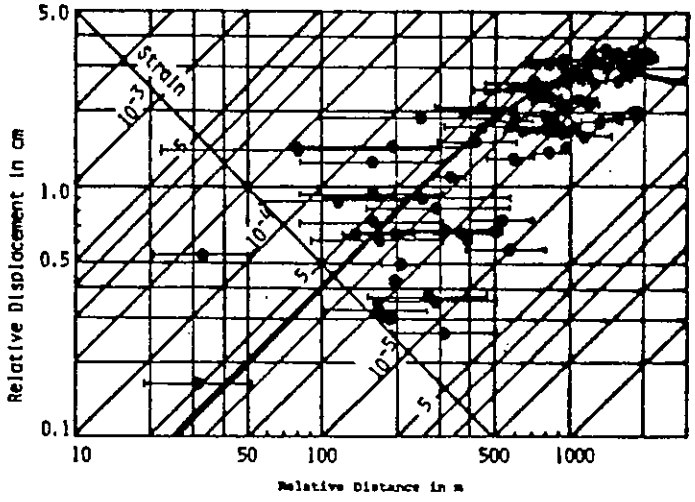

Fig. 5

Sample and Analytical Ground Deformation Spectra (N13°W Displacement, SMART-1, Event 5)